Chinese Physics Letters **42**, 024202 (2025) **Express Letter**

Optical Spiral Predator–Prey Dynamics

Juan Wu†, Yu-Hui Zhuang†, Yi Hu*, and Jing-Jun Xu*

The MOE Key Laboratory of Weak-Light Nonlinear Photonics, TEDA Applied Institute and School of Physics, Nankai University, Tianjin 300457, China

(Received 17 December 2024; accepted manuscript online 21 January 2025)

Chase-and-escape motion, which is a typical behavior between a predator and prey, is an important dynamics in animate systems. It has been concerned recently in optics aiming for achieving novel light steering and switching functions. However, this optical counterpart can be realized in only one dimension because of the challenges in maintaining the chase-and-escape interaction. Herein, we report, both theoretically and experimentally, the optical predator–prey dynamics in two dimensions for the first time. Upon nonreciprocal interaction, two beams can form a localized or oblique spiral chase-and-escape motion, which persists owing to the mutual light confinement. Unusual optical phenomena are observed in these dynamics: the angular momentum is not conserved and the resulting transverse traveling motion can be opposite to the applied initial momentum and enhanced by increasing the internal light interactions. The results can inspire further fundamental studies by exploring analogous animate phenomena in optics that are potentially useful for developing optical intelligence functions.

DOI: 10.1088/0256-307X/42/2/024202 CSTR: 32039.14.0256-307X.42.2.024202

1. Introduction. Chase-and-escape dynamics of predator and prey exist widely in living systems. They are seemingly unique in animal behaviors governed by the brain; however, they are unconsciously at play mediated by complex chemical processes, for instance,[1,2] at cellular levels or even smaller scales. Without considering the details of how and why they occur, these dynamics are equivalently described by a two-body model, where one object attracts the other, while the latter repels the former. This physical picture is essential in various types of collective motion in biological phenomena,[3–5] which further inspires people to synthesize predator–prey particles or droplets in inanimate matter,[6–10] aiming to achieve life-like adaptive organizations and functionalities.

In optics, light evolution exhibits similar predator–prey dynamics.[11–13] For instance, two optical pulses can accelerate in the same direction through their nonlinear interactions.[14–16] Such a scenario has a spatial counterpart in which the chase-and-escape behavior occurs transversely, manifesting as the co-deflection of two interacting light beams.[17] The underlying mechanism is analogous to that in a classic picture proposed for fuel-free propulsion,[18] where two objects with opposite mass signs tend to self-accelerate through their interactions.[19,20] The other way to realize optical chase-and-escape dynamics resorts to nonreciprocal light interactions: two light fields exert "forces" of the same direction to each other (via nonlinearly-induced refractive index changes), rather than following the action–reaction principle. In all previous studies, optical predator–prey dynamics were only realized in one dimension. One possible challenge in realizing its two-dimensional counterpart is that sufficient nonlinear interaction is prevented over a long distance by the self-defocusing nonlinearity experienced by one of the two interacting beams, which typically expands the beam and further weakens the nonlinear interactions.

In this study, we demonstrate, for the first time, both theoretically and experimentally, the predator–prey dynamics of two optical beams in two transverse dimensions via nonreciprocal light interactions. The beam expansion subject to self-defocusing nonlinearity in one beam is counteracted by the self-focusing nonlinearity experienced by the other beam, thereby providing sufficient strength of the nonlinear interaction for a long distance of evolution. The two beams can move spirally, with or without a transverse traveling motion, as determined by their initial tilts. In contrast to conventional optical spiral dynamics,[21,22] here the light interactions show nonconservation of the angular momentum. The spiral angle and velocity of the traveling motion could be tuned by altering the nonlinear strength.

2. Theory. In a two-body model describing natural predator–prey behaviors (for instance, a fox chases a rabbit), attraction and repulsion are manifested as the forces felt by the two bodies and point in the same direction [see Fig. 1(a)].[23,24] These forces are considered to be proportional to the separation between the predator and prey. Under these conditions, one can obtain the following motion equations: $m_{\mathrm{F,R}}\frac{d^2x_{\mathrm{F,R}}}{dt^2} = F_{\mathrm{F,R}}$, where m_{F} (m_{R}) and x_{F} (x_{R}) are mass and position, respectively, of a predator (prey) who feels a force F_{F} (F_{R}). A typical solution for these equations is shown in Fig. 1(a), where the two

†These authors contributed equally to this work.

*Corresponding author. Email: yihu@nankai.edu.cn; jjxu@nankai.edu.cn

© 2025 Chinese Physical Society and IOP Publishing Ltd. All rights, including for text and data mining, AI training, and similar technologies, are reserved.

bodies have zero velocity and their separation is initially nonzero. The two bodies undergo oscillatory dynamics, where the predator chases the prey. The key factor in realizing such dynamics is nonreciprocal interaction (i.e., the directions of the two interaction forces are the same), which can be realized in optics. For instance, one beam experiencing self-focusing nonlinearity induces a waveguide to attract the other beam, whereas the latter, experiencing self-defocusing nonlinearity, induces an anti-waveguide to repel the former. Subsequently, the two beams exhibit a chase-and-escape behavior.[20] In our study, we employ a realistic model that breaks the action–reaction principle effectively to study optical predator–prey dynamics, as shown below:

$$i\frac{\partial\varphi_{\mathrm{R}}}{\partial z} = -\frac{1}{2n_0k_0}\nabla_{\perp}^2\varphi_{\mathrm{R}} - k_0\Delta n\varphi_{\mathrm{R}}, \tag{1a}$$

$$i\frac{\partial\varphi_{\mathrm{F}}}{\partial z} = -\frac{1}{2n_0k_0}\nabla_{\perp}^2\varphi_{\mathrm{F}} - k_0\Delta n\varphi_{\mathrm{F}}, \tag{1b}$$

where φ_{R} and φ_{F} are complex amplitudes of two interacting optical beams, denoted as R-beam and F-beam that play the roles of a rabbit and a fox, respectively, $\nabla_{\perp}^2$ is Laplace operator, z is the propagation direction of the beams, k_0 is the wavenumber in vacuum, and n_0 is a linear refractive index. $\Delta n = \gamma\frac{|\varphi_{\mathrm{R}}|^2}{1+|\varphi_{\mathrm{R}}|^2} - \gamma\frac{|\varphi_{\mathrm{F}}|^2}{1+|\varphi_{\mathrm{F}}|^2}$ (γ is a nonlinear coefficient) is a nonlinear term that allows the R-beam and F-beam to feel self-focusing and defocusing nonlinearities, respectively. During nonlinear propagation, the F-beam tends to be delocalized owing to the self-defocusing nonlinearity, thus, weakening the light interactions. To maintain its localization, one can employ the waveguiding effect of the R-beam to confine it. The ideal condition is that the two beams are mutually confined to form a soliton. To solve soliton solutions, we assume $\varphi_{\mathrm{R}} = u_{\mathrm{R}}(x, y)\exp(i\delta_{\mathrm{R}}z)$ and $\varphi_{\mathrm{F}} = u_{\mathrm{F}}(x, y)\exp(i\delta_{\mathrm{F}}z)$, where δ_{R} and δ_{F} are eigenvalues. One typical solution is presented in Fig. 1(b) (simulation parameters are shown in Supplementary Materials). The R-beam is stronger than the F-beam to guarantee the wave-guiding effect to confine both the beams. Once the two components in the soliton are separated at the input, for instance, along the x-axis, they exhibit an oscillatory propagation similar to that of the particle model [Fig. 1(a)], as shown by their center of mass (defined by the expectation value of the position of an optical field) in Fig. 1(b). The forces $\bar{F}_{\mathrm{R}}$ and $\bar{F}_{\mathrm{F}}$ that are felt by the R-beam and F-beam, respectively, always point in the same direction. They are calculated using the negative derivation of the nonlinearly induced potential (i.e., $\bar{F}_{\mathrm{R,F}} = \frac{\langle\varphi_{\mathrm{R,F}}|-\nabla V|\varphi_{\mathrm{R,F}}\rangle}{\langle\varphi_{\mathrm{R,F}}|\varphi_{\mathrm{R,F}}\rangle}$, where $V = -k_0\Delta n$). Because of the intensity difference between the two beams, $\bar{F}_{\mathrm{F}}$ is larger than $\bar{F}_{\mathrm{R}}$. Thus, the F-beam can transversely surpass the R-beam, and then both slow down and start turning back upon the reversal of the interaction forces.

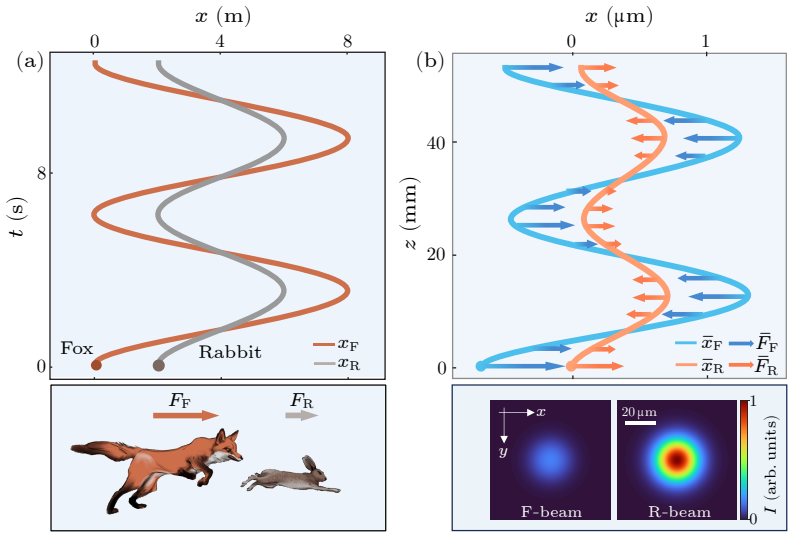

Fig. 1. Chase-and-escape dynamics in particle and (optical) wave models. (a) Trajectories of two particles representing a fox and a rabbit. (b) Center-of-mass ($\bar{x}_{\mathrm{F}}$ and $\bar{x}_{\mathrm{R}}$, upper row) of two mutually-confined optical beams (bottom row) along the propagation distance. The arrows present the forces felt by the particles/beams, and their orientation and length characterize the direction and magnitude of the force, respectively. Both models show oscillatory motions under similar initial conditions: two entities have zero velocity and a nonzero separation.

Once an initial momentum is applied to the two beams, being misaligned with the direction along which they separate, spiral dynamics are induced. Figure 2 presents three typical trajectories (tracing the center of mass of the beams, i.e., $\bar{r}_{\mathrm{R}}$ and $\bar{r}_{\mathrm{F}}$) initiated by tilting the R- and/or F-beams (accordingly introducing a transverse wave vector ($k_{\perp}$) along the positive y-axis). For both beams with proper initial tilts, the beams are dynamically localized, performing a quasi-circular motion in the x–y plane [Fig. 2(a)], where the interaction forces play the role of centripetal forces. To fit nonreciprocal interactions, the transverse wave vectors should point in the same direction at the input. Subsequently, the two beams rotate to nearly identical azimuthal positions in the following propagation.

If only one beam is tilted at the input, an oblique spiral dynamics occurs, exhibiting a traveling motion transversely [Figs. 2(b) and 2(c)]. The orientation of the spiral trajectory is similar to the initial tilt of the R-beam [Fig. 2(b)]. Accordingly, the transverse traveling motion points to the positive y-axis, which is triggered by the positive y-components of the forces felt by the two beams at the propagation onset. Its moving direction is maintained by inertia in the subsequent propagation, even if the y-components of the forces become negative. Eventually, the two beams have a net increment of displacement in the positive y-axis when the R-beam returns to the left (i.e., towards the negative x-axis) of the F-beam and both are ready to repeat another round of spiral motion. In the case where only the F-beam is tilted, the transverse traveling motion is reversed in the direction of the initially applied momentum [Fig. 2(c)], causing a counterintuitive orientation of the oblique spiral trajectory. Upon the initial tilt, the F-beam tends to rotate clockwise around the R-beam. Subsequently, both beams experience internal forces with components pointing in the negative y-axis at the early stage of propagation; thus, the spiral dynamics are against the initial momentum. It should be noted that these spiral motions are difficult to achieve in the absence of mutual beam confinement because the self-defocusing nonlinearity experienced by the F-beam tends to delocalize this beam significantly, thereby largely reducing the light interactions and consequently disabling the chase-and-escape motion.[16] This difficulty is also encountered when using the mechanism associated with opposite mass signs, as the two beams subject to the chase-and-escape motion tend to separate rather than overlapping. Additional simulations without mutual beam confinement are provided in the Supplementary Materials.

In the optical spiral predator–prey dynamics, the total angular momentum ($\bar{L}_z$) of the two beams is found to be nonconserved, as shown by the values presented in the panels of x–y plane in Fig. 2 (details are provided in the Supplementary Materials). The angular momentum exhibits a large variance along the propagation when only one beam is initially tilted. However, the change is quite small for quasi-circular dynamics. In exact circular motion, the angular momentum is constant. However, this ideal case is difficult to achieve because of the wave nature of light. In principle, the nonoverlapping of the two soliton components causes a variance in the beam profile during propagation, which prevents the interaction forces from being constant. The wave–particle difference is observed in the deviation of the trajectory, plotted based on a model assuming that the two components do not change along the propagation (indeed becoming a particle model, see Supplementary Materials), as presented in the rightmost panels of Fig. 2.

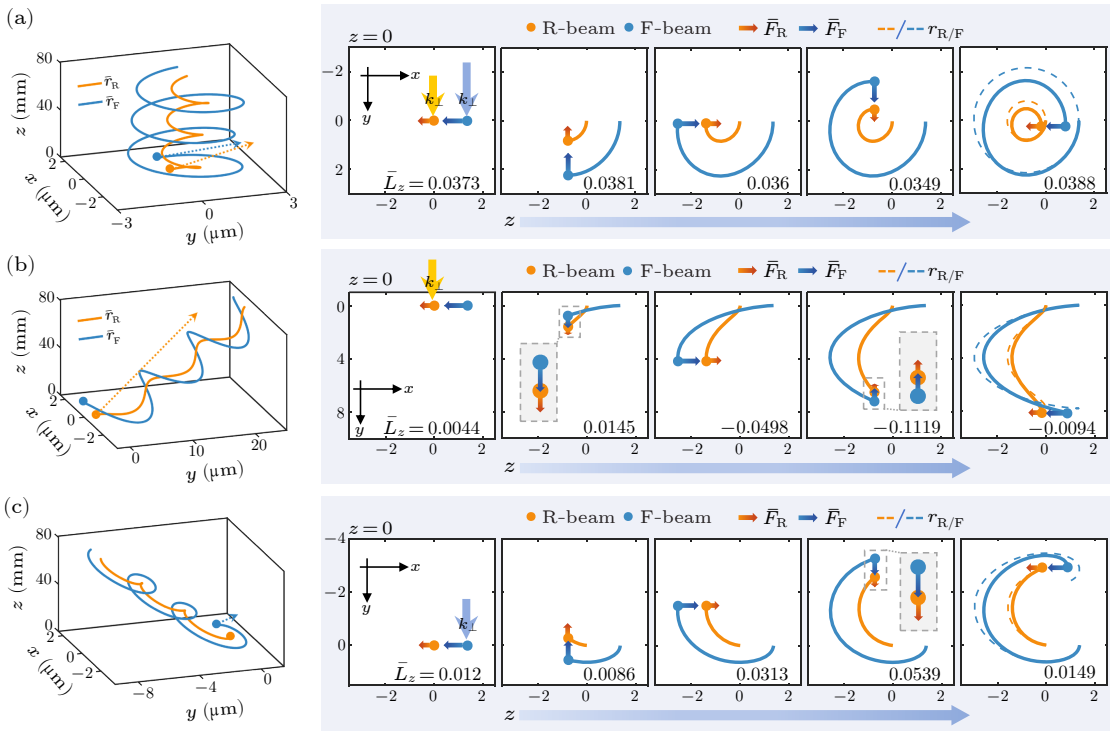

Fig. 2. Simulated spiral chase-and-escape dynamics of two optical beams. (a)–(c) Trajectories (solid, center-of-mass) of the beams during propagation and their projection at different distances of equal spacing in the transverse dimension (i.e., x–y plane) for the cases of that (a) both beams, (b) only R-beam, or (c) only F-beam have initial tilts. Other beam parameters at the input are the same for the three cases. The straight dotted lines in the leftmost panels are trajectories of the tilted beams during linear propagation. In the panels of x–y projection, the forces felt by the beams are characterized by the vector features of arrows, and the value of the total angular momentum is listed at bottom-right corner. For comparison, the trajectories (dashed) solved by employing a particle model with the same input conditions are plotted in the rightmost panels.

3. Experiment. To verify the optical spiral predator–prey behaviors, we used the experimental setup schematically plotted in Fig. 3(a) (details are provided in the Supplementary Materials). R-beam and F-beam were stroboscopic optical beams obtained by employing a digital micromirror device (DMD) to amplitude-modulate a continuous-wave (CW) laser temporally and periodically. Therefore, two blank masks with different grey values were played in a loop in the DMD. The R- and F-beams were modulated individually by a spatial light modulator (SLM) that was synchronized well with the DMD. Using these programmable devices, the intensity profiles, tilts, and spacings of the two beams could be easily adjusted. The optical nonlinearity in our setup was achieved by applying an alternating current (AC) voltage to a strontium barium niobate (SBN) crystal. An R-beam (F-beam) was injected into the crystal during a period of positive (negative) voltage; thus, experiencing self-focusing (defocusing) nonlinearity. Because of the storage properties of the crystal (i.e., the light-induced refractive index changes did not disappear instantaneously when the illuminating light was switched off), the two beams could interact with each other, although they were not in the medium simultaneously. This nonlinear interaction could be approximately regarded as a real-time process because the storage time of the crystal was considerably longer than the switching time of the two beams (see Supplementary Materials). The beam intensity profiles at the crystal output were recorded using a charge-coupled device (CCD) and a lens.

To achieve persistent interaction, R-beam and F-beam should be mutually confined, as aforementioned. Such confinement was studied by overlapping the two beams (imparted with similar Gaussian profiles) without spacing [Figs. 3(b) and 3(c)]. When the power ratio between the R-beam and F-beam was 256:50 and the amplitude of the AC voltage applied to the crystal was 300 V, the two beams exhibited localization along the propagation [Figs. 3(d)–3(g)], in stark contrast to their linear expansion owing to diffraction [Figs. 3(h) and 3(i)]. The elliptical features shown in the intensity pattern were caused by the anisotropy of the nonlinearity in the crystal and the elliptical shape of the injected beams (as shown by their linear diffraction patterns). Although the two beams were not ideally invariant during propagation, their mutual confinement was sufficient for observing a persistent nonreciprocal light interaction, as shown below.

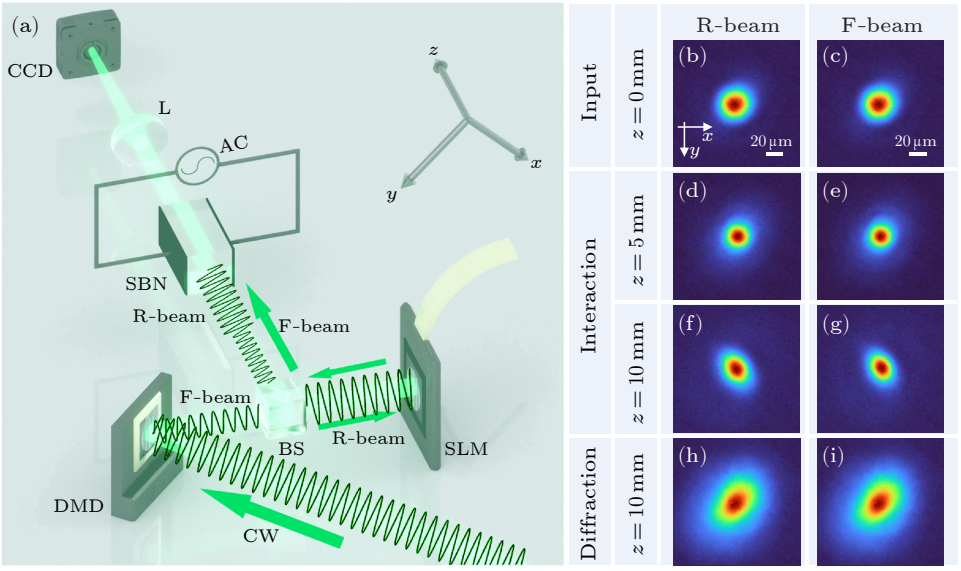

Fig. 3. Realization of two mutually confined optical beams. (a) Schematic experimental setup: R-beam and F-beam experience self-focusing and -defocusing nonlinearities at different time periods, respectively, and they interact via the storage property of the SBN crystal. (b)–(i) Measured intensity patterns (normalized) of R-beam (left column) and F-beam (right column) at different propagation distances for the cases of (b)–(g) nonlinear interactions and (h), (i) linear diffraction. In these measurements, the two beams almost overlap in the spatial domain.

To perform the predator–prey experiment, the two beams presented in Fig. 3 were separated by a distance of ∼12 μm in the x-axis at the input; meanwhile, one of them was applied with an initial tilt downwards (i.e., the transverse wave vector is along the positive y-axis). Upon interaction, they undergo counterclockwise and clockwise spiral propagations, as shown in Figs. 4(a) and 4(b), respectively. The change in the rotation angle from $z = 5$ to 10 mm was close to that from $z = 0$ to 5 mm, similar to the simulation where the angle change was nearly linear with distance (note that the x–y panels in Fig. 2 are equally spaced along the z-axis). As the nonlinear interaction was strengthened by increasing the amplitude of the applied voltage to 400 V, the rotation angle increased [Figs. 4(c) and 4(d)]. This is in accordance with the fact that the angular frequency is positively related to the centripetal force. When the voltage amplitude further increased (to 500 and 600 V), the rotation angle tended to increase at $z = 5$ mm but decreased at $z = 10$ mm with the strengthening of the nonlinear interaction. Under these conditions,

a large part of the F-beam tended to not participate in the nonlinear interaction owing to the self-defocusing nonlinearity, particularly at the rear propagation, thereby leading to a slowdown in the rotation. By altering the input beam parameters, larger rotation angles could be achieved (see Supplementary Materials). In both spiral dynamics, the two beams showed a vertical traveling movement [Figs. 4(e) and 4(f)], characterized by a change in their total center of mass in the y-axis, that is, $\Delta\bar{y}_{\text{total}}$ (calibrated by the self-deflection effect owing to diffusion nonlinearity in the SBN crystal). For the case of tilting R-beam only, the two beams moved downwards as a whole, following the direction of the initial tilt. However, such a movement is reversed when only the F-beam has an identical tilt, as predicted in the simulations shown in Fig. 2. As the voltage amplitude (accordingly, the nonlinear interaction) was increased, the beam displacement associated with the vertical movement was enhanced in the latter case, yet had a slight change in the former case.[25] This difference stemmed from the anisotropy of the crystals. As a reference, the beam displacement was also increased with the voltage amplitude by simply switching the two beams at the input in the case of tilting the R-beam only [Fig. 4(e)]. The observed enhancement of the traveling motion offers additional evidence that the internal interaction can contribute to the movement of the two beams as a whole. It should be noted that circular spiral dynamics were hardly realized in the current setting, where the anisotropic nonlinearity in the crystal did not offer a constant beam interaction that could act as a centripetal force.

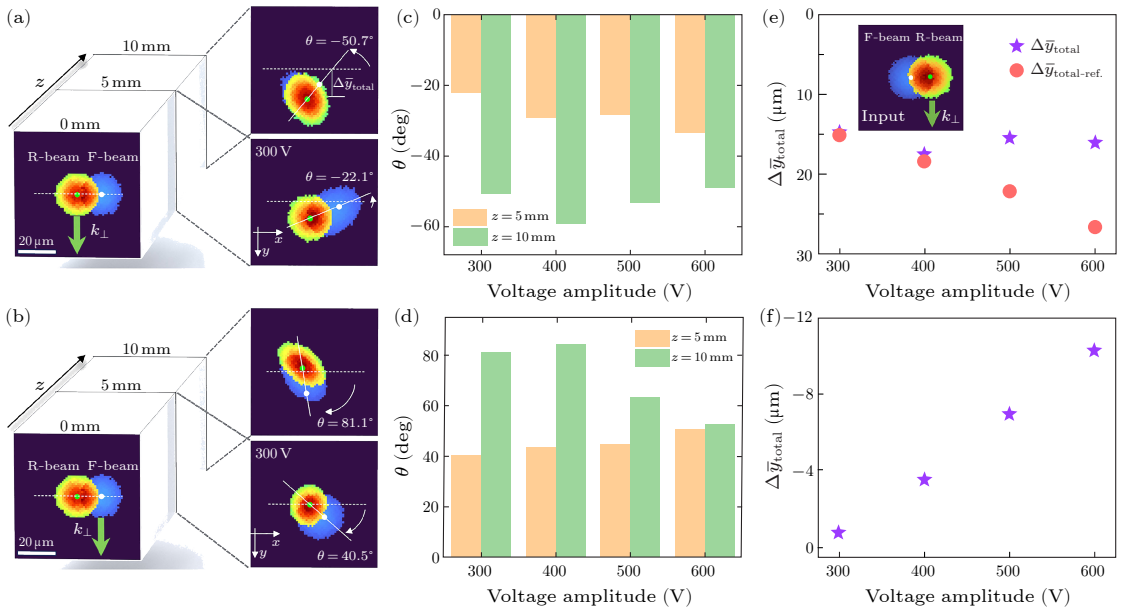

Fig. 4. Spiral chase-and-escape motion of two optical beams in experiment. Upper and bottom rows correspond to the cases of tilting only R- and F-beam at the input, respectively. (a) and (b) present measured beam patterns at different propagation distances. Other input conditions, including the profiles and spacing of the two beams are the same. Green (white) dots are the center-of-mass of R- (F-) beams. Each beam pattern is plotted by a cutoff of the parts below the half of its peak intensity to better show the relative position of the two beams. (c) and (d) The rotation degree (i.e., θ) of F-beam around R-beam and (e), (f) displacement of the two beams as a whole along the y-axis with different applied voltages. In (e), the beam displacement for the case of switching the two beams in (a) at the input is presented for reference.

4. Conclusion. We demonstrated, for the first time, the spiral predator–prey dynamics of two optical beams using nonreciprocal light interactions. The realization of these dynamics is attributed to mutual beam confinement that maintains beam localization to provide persistent nonlinear interaction strength. Localized (quasi-circular) motion is formed by properly tilting both beams, whereas an oblique spiral dynamics is generated by tilting only one beam, carrying a transverse traveling motion that follows or reverses the direction of the initial beam momentum. All dynamics show nonconservation of the angular momentum. The main features of predator–prey dynamics are observed on an optical platform. We further observe that the transverse beam displacement in oblique spiral dynamics increases with the increase in the beam interactions, which evidently supports the idea that the internal interactions contribute to the entire motion of the two beams. These results pave the way for building a link between light and active matter, based on which optical self-organization is envisioned for the realization of novel optical functions. Additionally, more intriguing dynamics can be expected by introducing the polarization of light as another degree of freedom in these nonlinear interactions. Polarization may be used to tune spiral trajectories as well as generate fruitful collective effects arising from predator–prey dynamics.

Acknowledgements. This work was supported by the National Key R&D Program of China (Grant No. 2022YFA1404800), the National Natural Science Foundation of China (Grant Nos. 12250009 and 62075105),

and the 111 Project in China (Grant No. B23045).

References

[1] Sengupta A, Kruppa T, and Löwen H 2011 *Phys. Rev. E* **83** 031914
[2] Hamilton P T, Anholt B R, and Nelson B H 2022 *Nat. Rev. Immunol.* **22** 765
[3] Nagy M, Ákos Z, Biro D, and Vicsek T 2010 *Nature* **464** 890
[4] Vicsek T and Zafeiris A 2012 *Phys. Rep.* **517** 71
[5] Cohen Y, Pasternak Z, Muller S, Hubschmann T, Schattenberg F, Sivakala K K, Abed-Rabbo A, Chatzinotas A, and Jurkevitch E 2021 *Nat. Commun.* **12** 5481
[6] Usta O B, Alexeev A, Zhu G, and Balazs A C 2008 *ACS Nano* **2** 471
[7] Schmidt F, Liebchen B, Löwen H, and Volpe G 2019 *J. Chem. Phys.* **150** 094905
[8] Meredith C H, Moerman P G, Groenewold J, Chiu Y J, Kegel W K, van Blaaderen A, and Zarzar L D 2020 *Nat. Chem.* **12** 1136
[9] Mou F, Li X, Xie Q, Zhang J, Xiong K, Xu L, and Guan J 2020 *ACS Nano* **14** 406
[10] Li Z, Li H, Li A, Liu Z, Zhang Z, Li K, Qiao Y, and Song Y 2021 *Adv. Mater. Interfaces* **8** 2101309
[11] Batz S and Peschel U 2013 *Phys. Rev. Lett* **110** 193901
[12] Wimmer M, Regensburger A, Bersch C, Miri M-A, Batz S, Onishchukov G, Christodoulides D N, and Peschel U 2013 *Nat. Phys.* **9** 780
[13] Zhang P, Hu Y, Bongiovanni D, Li Z, Morandotti R, Chen Z, and Xu J 2021 *Phys. Rev. Lett.* **127** 083901
[14] Pei Y, Hu Y, Lou C, Song D, Tang L, Xu J, and Chen Z 2018 *Opt. Lett.* **43** 118
[15] Pei Y, Hu Y, Zhang P, Zhang C, Lou C, Rüter C E, Kip D, Christodoulides D, Chen Z, and Xu J 2019 *Opt. Lett.* **44** 5949
[16] Pei Y, Wang Z, Hu Y, Lou C, Chen Z, and Xu J 2020 *Opt. Lett.* **45** 3175
[17] Millis M G 1997 *J. Propul. Power* **13** 577
[18] Bondi H 1957 *Rev. Mod. Phys.* **29** 423
[19] Alberucci A, Jisha C P, Peschel U, and Nolte S 2019 *Phys. Rev. A* **100** 011802
[20] Ma W, Zhuang Y, Wang Z, Jia P, Zhang P, Hu Y, Chen Z, and Xu J 2022 *Laser Photonics Rev.* **17** 2200177
[21] Shih M F, Segev M, and Salamo G 1997 *Phys. Rev. Lett.* **78** 2551
[22] Stepken A, Belić M R, Kaiser F, Królikowski W, and Luther-Davies B 1999 *Phys. Rev. Lett.* **82** 540
[23] Sprott J C 2009 *Am. J. Phys.* **77** 783
[24] Zhdankin V and Sprott J C 2010 *Phys. Rev. E* **82** 056209
[25] Zhang P, Lou C, Hu Y, Liu S, Zhao J, Xu J, and Chen Z 2012 *Nonlinear Photonics and Novel Optical Phenomena* (New York: Springer) p. 133